Journal of Biomedical Optics

BiomedicalOptics.SPIEDigitalLibrary.org

Miniature fiber optic spectrometer-based quantitative fluorescence resonance energy transfer measurement in single living cells

Liuying Chai
Jianwei Zhang
Lili Zhang
Tongsheng Chen

SPIE.

Miniature fiber optic spectrometer-based quantitative fluorescence resonance energy transfer measurement in single living cells

Liuying Chai, Jianwei Zhang, Lili Zhang, and Tongsheng Chen*
South China Normal University, College of Life Science, Institute of Laser Life Science, MOE Key Laboratory of Laser Life Science, Guangzhou 510631, China

Abstract. Spectral measurement of fluorescence resonance energy transfer (FRET), spFRET, is a widely used FRET quantification method in living cells today. We set up a spectrometer-microscope platform that consists of a miniature fiber optic spectrometer and a widefield fluorescence microscope for the spectral measurement of absolute FRET efficiency (E) and acceptor-to-donor concentration ratio (R_C) in single living cells. The microscope was used for guiding cells and the spectra were simultaneously detected by the miniature fiber optic spectrometer. Moreover, our platform has independent excitation and emission controllers, so different excitations can share the same emission channel. In addition, we developed a modified spectral FRET quantification method (mlux-FRET) for the multiple donors and multiple acceptors FRET construct ($mD \sim nA$) sample, and we also developed a spectra-based 2-channel acceptor-sensitized FRET quantification method (spE-FRET). We implemented these modified FRET quantification methods on our platform to measure the absolute E and R_C values of tandem constructs with different acceptor/donor stoichiometries in single living Huh-7 cells. [DOI: 10.1117/1.JBO.20.3.037008]

Keywords: resonance energy transfer; quantitative fluorescence resonance energy transfer measurement; spectral unmixing; living cells; miniature fiber optic spectrometer; fluorescence microscopy; multiple donors and multiple acceptors fluorescence resonance energy transfer construct.

Paper 140779R received Nov. 25, 2014; accepted for publication Feb. 16, 2015; published online Mar. 20, 2015.

1 Introduction

Fluorescence resonance energy transfer (FRET) has become an important tool for the analysis of intracellular biological processes[1] and biological sensor applications.[2] Recent publications have shown that a multiple acceptors-based FRET technique has the potential to characterize the functions of multiprotein complexes in living cells and the spatial conformation of macromolecules on a scale larger than 10 nm.[3,4] Multiple acceptors interacting with the same donor increase the probability of FRET even without a change in molecular distance and thus lead to high transfer efficiency.[5] For example, FRET constructs with one donor and 10 acceptors can be used to determine distances as long as 20 nm.[6] It was found that the amount of energy transfer observed in constructs with multiple acceptors ($1D \sim nA$, "D" denotes donor molecule and "A" denotes acceptor molecule, n represents the number of acceptors in the FRET construct) is significantly greater than the FRET efficiency predicated from the sum of the individual donor to acceptor transfer rates, indicating that either an additional energy transfer pathway exists when multiple acceptors are present or the theoretical assumption on which the kinetic model prediction is based is incorrect.[7]

Although FRET microscopy has become an important tool for monitoring intracellular biological processes, the contamination of spectral crosstalks, including donor emission crosstalk and acceptor excitation crosstalk, restricts the live cell applications of FRET.[1,8] FRET quantification is very important for the quantitative comparison between different laboratories and/or cells with different expression levels of fluorescent proteins (FPs).[8–11] Fluorescence lifetime imaging microscopy (FLIM), acceptor photobleaching (PbFRET), and acceptor-sensitized emission (SE-FRET) methods have been developed for FRET quantification.[8] FLIM and PbFRET methods cannot provide the information about acceptor-to-donor concentration ratio (R_C), and the long measurement time and irreversible destruction of photobleaching make the two methods incompatible with time-lapse live cell applications.[8,12–14]

SE-FRET method, the most widely used approach for dynamic live cell FRET applications,[8] includes 3-cube-based methods such as E-FRET and spectral unmixing method (spFRET).[9–11,15–19] The nondestructive nature (in contrast to the popular PbFRET technique) and the sensitivity even at high acquisition speed (in contrast to the fluorescence lifetime imaging) make E-FRET the method of choice for measurements over extended periods of time.[8] spFRET is based on the axiom that the net fluorescence spectrum is defined by the linear superposition of the spectra for each fluorophore in the sample.[19] Lux-FRET, a representative spFRET method developed by Wlodarczyk et al.,[17] can resolve both the apparent FRET efficiency (E_{app}) and R_C for the FRET sample in the presence of free donors and acceptors.[11] Both E-FRET and Lux-FRET methods require at least three reference samples separately expressing donor-only, acceptor-only, and donor-acceptor

*Address all correspondence to: Tongsheng Chen, E-mail: chentsh@scnu.edu.cn or chentsh126@126.com

1083-3668/2015/$25.00 © 2015 SPIE

tandem construct for calibrations, and all experiments for references and FRET samples must be performed under the same measurement conditions.[9,15,17]

E-FRET can be implemented on widefield and confocal microscopes.[8,20] Considering the stability of widefield microscopes and the low cost, E-FRET is generally implemented on widefield microscopes.[1,9,15,21] However, it is generally difficult to choose an appropriate optical filter as a donor emission channel to selectively collect donor emission, a requirement of an E-FRET method,[9,15] for some FPs pairs such as green fluorescent protein (GFP) and yellow fluorescent protein (YFP).[22] FRET quantification in single living cells by spFRET is generally implemented on a confocal microscope with spectral detectors (Zeiss 510 META, Zeiss 710/780, Olympus FV 1000/1200, Leica TCS SP2/5/8, and Nikon A1).[11] There are two spectral acquisition modes for confocal microscopes:[23] (1) synchronization acquisition of multiband spectra with about 10-nm spectral resolution,[16,24] which is useful for multispectral imaging of rapid processes in living cells.[17] However, fewer data points may limit the accuracy when spectrally unmixing signals from the FRET sample;[25] (2) time-lapse acquisition of multiband spectra with about 2-nm spectral resolution,[26] which needs a long detection time.

In this report, for the first time, we combine a miniature fiber optic spectrometer and a widefield fluorescence microscope to perform spectral measurement of FRET quantification in single living cells. This platform has two specialties: (1) independent excitation and emission controllers; (2) simultaneous microscopic imaging and spectral detection. In addition, we developed a modified spFRET method, mlux-FRET, for quantifying the multiple donors and multiple acceptors system ($mD \sim nA$ construct, m represents the number of donors in the FRET construct) in the presence of free donors and acceptors and a spectra-based 2-channels E-FRET (spE-FRET) method for quantifying the $mD \sim nA$ FRET construct. Finally, we implemented these modified FRET quantification methods on our platform to measure the absolute FRET efficiency (E) and acceptor-to-donor concentration ratio (R_C) of tandem constructs with different acceptor/donor stoichiometries in single living Huh-7 cells.

2 Experimental Setup

Figure 1(a) depicts the schematic of this platform which consists of a widefield fluorescence microscope (Axio Observer, Carl Zeiss, Oberkochen, Germany) and two detection channels: a spectral detection channel and a CCD imaging channel. The excitation light source is a metal halide lamp (X-Cite 120, Carl Zeiss, Oberkochen, Germany), and its intensity can be attenuated in five discrete steps (TC1, transmission controller) ($T_1 =$ 0%, 12.5%, 25%, 50%, and 100%), and another neutral density filters' controller (TC2) with six discrete steps ($T_2 = 2\%$, 20%, 40%, 60%, 80%, and 100%) can be used for the same purpose. Collimated light from the lamp first transmits through an excitation controller (EC) with three filters. In our study, two excitation bandpass filters of BP 405/20 (Ex405 nm) (BP 405/20× Exciter, Chroma) and BP 436/20 (Ex436 nm) (BP 436/20, Carl Zeiss, Oberkochen, Germany) were installed in the No. 1 and No. 2 positions, respectively, and the No. 3 position is empty.

An objective (40 × /1.3 NA oil) is used to focus the illumination light into the sample, and emission is collected through the same objective and sent back into the same dichroic mirror (DM) and a long-pass (LP) filter. We chose here a primary DM of FT 455 (455DCLP Dichroic, Chroma) and an emission LP filter of LP 455 (455DCLP Dichroic, Chroma) as emission control. Fluorescence reflected by the mirror first passes through a detection controller (DC), and then through a cooled CCD camera (AxioCam MRm, Carl Zeiss, Oberkochen, Germany) and/or a miniature fiber optic spectrometer (QE65 Pro, Ocean Optics, Florida). The DC has three detection modes: (1) microscopic imaging by CCD channel that operates as a guidance for finding the cells; (2) spectral detection by spectrometer channel; (3) simultaneous microscopic imaging and spectral detection. For our spectrometer-microscope platform, the EC is independent of the emission controller, thus we can get two different combinations of excitation and emission filters by adjusting EC, which is very important for the rapid measurement of two excitation wavelengths-based spFRET methods.

The miniature fiber optic spectrometer (QE65 Pro) is a compact and flexible system without moving parts, and can be readily connected to a widefield microscope with an interfacing

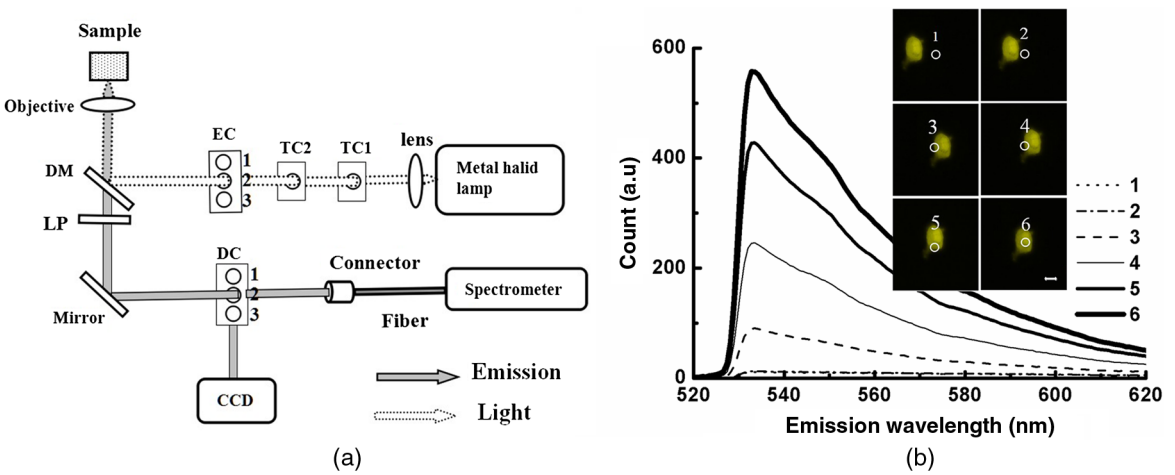

Fig. 1 (a) Optical setup. CCD: CCD imaging channel; spectrometer: spectrometer detection channel; TC1: transmission controller1; TC2: transmission controller 2; EC: excitation controller; DM: dichroic mirror; LP: long-pass filter; DC: detection controller with three modes: reflector mirror (1), empty (2), and beam splitter mirror (3). (b) Count spectra of a living Huh-7 cell expressing YFP-Bax at different positions (inset figure) with 500-nm excitation. White circle area: the detection area of the spectrometer. Scale bar: 10 μm.

connection type C. The detector used in QE65 spectrometer is a back-thinned, 1044×64 element CCD array, and the spectral detection range is 221.705 to 1015.805 nm. Each count(λ) at the emission wavelength λ recorded by singe column pixels (64 pixels) of the QE65 spectrometer is related to the photons from about a 0.761-nm wavelength range. In our study, the diameter (d) of the fiber (QP600-2-UV-VIS, Ocean Optics, Florida) is 600 μm.

The effective imaging area of a CCD camera with a pixel resolution of 692×520 (2×2) is about 5.988×107 μm^2 and the corresponding imaging sample area is about 1.46×10^4 μm^2. We first installed the same two CCD cameras on the two detection channels to collimate them using a standard fluorescence sample, and then replaced one CCD camera with the interfacing connection type C of the spectrometer. The detection area (S) of the spectrometer is: $S=\pi(d/2)^2=2.826\times10^5 \mu m^2$ corresponding to the 68.99 μm^2 of the sample area. Figure 1(b) showed the count spectra of a Huh-7 cell expressing YFP-Bax at different positions (inset figures) with 500-nm excitation. When the cell was centered in the CCD channel, the corresponding fluorescence intensity collected by the spectrometer was the maximum, indicating that the detection area of the spectra channel concurs with the middle of the CCD imaging channel.

In our experiments, fluorophores were excited by 405 or 436 nm ($T = T_1 \times T_2 = 12.5\% \times 20\% = 2.5\%$) excitation. We also used a 500 nm ($T = T_1 \times T_2 = 50\% \times 100\% = 50\%$) excitation with the combination of an excitation bandpass filter of BP 500/25 (Ex500 nm) (BP 500/25, Carl Zeiss, Oberkochen, Germany), primary DM FT 515 (BP 500/25, Carl Zeiss, Oberkochen, Germany), and emission bandpass filter of BP 535/30 (BP 535/30, Carl Zeiss, Oberkochen, Germany) to bleach the acceptor. The fluorescence intensity is collected in the spectra range of 460 to 620 nm.

3 DNA Constructs and Cells

3.1 *Reagent and Plasmids*

Cerulean, Venus-kras, and YFP-Bax plasmids were purchased from Addgene Company (Cambridge, Massachusetts). The FRET-standard constructs, including Cerulean-32-Venus (C32V, Addgene plasmid 29396), Cerulean-5-Venus-5-Cerulean (CVC, Addgene plasmid 27788), Venus-5-Cerulean-5-Venus (VCV, Addgene plasmid 27788), and Venus-5-Cerulean-5-Venus-6-Venus (VCVV, Addgene plasmid 27789), were kindly provided by the Vogel lab (National Institutes of Health, Bethesda, Maryland).

3.2 *Cell Culture and Transfection*

Huh-7 cells, a human hepatocellular carcinoma cell line, were obtained from the Department of Medicine, Jinan University, Guangzhou, China. Cells were cultured in Dulbecco's modified Eagle's medium (DMEM, Gibco, Grand Island, New York) containing 10% fetal calf serum (FCS; Sijiqing, Hangzhou, China) at 37°C under 5% CO_2 in a humidified incubator. For transfection, cells were cultured in DMEM containing 10% FCS in a 35-mm glass dish with a density of 4×10^4 cells/ml at 37°C under 5% CO_2 in a humidified incubator. After 24 h, when the cells reached about 70% to 90% confluence, plasmid was transfected into the Huh-7 cells for 24-48 h. Turbofect™ (Fermentas Inc., Glen Burnie, Maryland) was used as a transfection reagent.

3.3 *Statistical Analysis*

Results are expressed as mean ± SD. Data were analyzed by repeated measures ANOVA with parametric methods using the statistical software SPSS 18.0 (SPSS, Inc., Chicago, Illinois). Throughout the work, P values less than 0.05 were considered to be statistically significant.

4 FRET Quantification Methods

Throughout the paper, count $i(\lambda)$ denotes the measured count spectrum recorded by the spectrometer at specific measurement conditions, and the superscript number i denotes the excitation wavelength λ^i; subscript capital letter X denotes the experimental sample ("D" denotes the donor sample; "A" denotes the acceptor sample, and space denotes the FRET sample).

4.1 *mlux-FRET: Modified lux-FRET Theory*

With two excitation wavelengths, lux-FRET can simultaneously measure the absolute E and R_C of the FRET samples including $D \sim A$ FRET constructs and free donors and acceptors.[11,17] In addition, for the time-invariant and uniform acceptor/donor ratio such as the tandem construct sensors, after an initial spectrally resolved dual-excitation calibration, the user can perform repetitive single-excitation wavelength measurements to quantify E at high temporal resolution.[11,17] Here, we developed a modified lux-FRET method, mlux-FRET, to measure the absolute E and R_C of the FRET samples including $mD \sim nA$ FRET constructs, free donors, and acceptors. Considering an FRET sample containing $mD \sim nA$ FRET constructs, free donors, and free acceptors, the emission spectra should be a linear combination of five contributions from the free donor, the donor in $mD \sim nA$ FRET constructs, the free acceptor and the acceptor in $mD \sim nA$ FRET constructs including direct excitation and sensitized emission:

$$\mathrm{count}^i(\lambda) = f(\lambda)\left\{\begin{array}{l} I^i\eta^i(\lambda)(\varepsilon_D^i Q_D e_D(\lambda)[D] + \varepsilon_D^i Q_D e_D(\lambda) m[mD \sim nA])(1-E) + \varepsilon_A^i Q_A e_A(\lambda)[A] \\ +\varepsilon_A^i Q_A e_A(\lambda) n[mD \sim nA] + \varepsilon_D^i Q_A e_A(\lambda) m[mD \sim nA]E) \end{array}\right\}, \quad (1)$$

where $f(\lambda)$ is the transfer factor of the spectrometer from fluorescence intensity to count at the emission wavelength λ; E is the FRET efficiency of $mD \sim nA$ FRET construct; I^i is the illumination intensity at λ^i excitation; $\eta^i(\lambda)$ is the detection efficiency of the instrument used; ε_D^i and ε_A^i are the extinction coefficients of the donor and acceptor at λ^i excitation; Q_D and Q_A are the quantum yields of the donor and acceptor; $e_D(\lambda)$ and $e_A(\lambda)$ are the spectral fingerprints of the donor and acceptor normalized to unit area; $[D]$ and $[A]$ are the concentrations of free donors and acceptors in the FRET sample; $[mD \sim nA]$ is the concentration of $mD \sim nA$ constructs.

Sorting these terms in Eq. (1) according to those with emission characteristics of the donor and acceptor, respectively, we obtain

$$\begin{aligned}\text{count}^i(\lambda) &= f(\lambda)I^i\eta^i(\lambda)\begin{pmatrix}\varepsilon_D^i Q_D e_D(\lambda)([D]+(1-E)m[mD\sim nA])+\varepsilon_A^i Q_A e_A(\lambda)([A]\\ +\left(n+mE\frac{\varepsilon_D^i}{\varepsilon_A^i}\right)[mD\sim nA]\end{pmatrix}\\ &= \frac{([D]+(m-mE)[mD\sim nA])}{[D^{\text{ref}}]}\text{count}_D^{i,\text{ref}}(\lambda)+\frac{\left([A]+\left(n+mE\frac{\varepsilon_D^i}{\varepsilon_A^i}\right)[mD\sim nA]\right)}{[A^{\text{ref}}]}\text{count}_A^{i,\text{ref}}(\lambda),\end{aligned} \tag{2}$$

where $\text{count}_D^{i,\text{ref}}(\lambda)$ and $\text{count}_A^{i,\text{ref}}(\lambda)$ are the reference count spectra obtained from cells separately expressing donors with concentration $[D^{\text{ref}}]$ and acceptors with concentration $[A^{\text{ref}}]$, respectively, under the same measurement conditions as the FRET samples:

$$\text{count}_D^{i,\text{ref}}(\lambda) = f(\lambda)I^i\varepsilon_D^i Q_D\eta^i(\lambda)e_D(\lambda)[D^{\text{ref}}], \tag{3}$$

$$\text{count}_A^{i,\text{ref}}(\lambda) = f(\lambda)I^i\varepsilon_A^i Q_A\eta^i(\lambda)e_A(\lambda)[A^{\text{ref}}]. \tag{4}$$

We define two apparent relative donor and acceptor concentrations, respectively, as follows:

$$\delta^i = \frac{[D]+(m-mE)[mD\sim nA]}{[D^{\text{ref}}]}, \tag{5}$$

$$\alpha^i = \frac{[A]+(n+mE\varepsilon_D^i/\varepsilon_A^i)[mD\sim nA]}{[A^{\text{ref}}]}, \tag{6}$$

and Eq. (2) becomes:

$$\text{count}^i(\lambda) = \delta^i\text{count}_D^{i,\text{ref}}(\lambda)+\alpha^i\text{count}_A^{i,\text{ref}}(\lambda). \tag{7}$$

We can obtain the corresponding excitation ratio ($r^{\text{ex},i}$) at λ^i excitation from the reference measurements [Eqs. (3) and (4)]

$$r^{\text{ex},i} = \frac{\text{count}_D^{i,\text{ref}}(\lambda)Q_A e_A(\lambda)}{\text{count}_A^{i,\text{ref}}(\lambda)Q_D e_D(\lambda)} = \frac{\varepsilon_D^i}{\varepsilon_A^i}\frac{[D^{\text{ref}}]}{[A^{\text{ref}}]}. \tag{8}$$

Considering two different excitation wavelengths, Eqs. (5) and (6) represent three independent equations [since Eq. (5) does not rely on the extinction coefficient ratio $\gamma^i = \varepsilon_D^i/\varepsilon_A^i$]. From Eqs. (5), (6), and (8), we can obtain the apparent efficiency (E_{app}) and R_C:

$$Ef_D = E\frac{m[mD\sim nA]}{[D^t]} = \frac{\Delta\alpha}{\Delta r\delta^1+\Delta\alpha}, \tag{9}$$

$$Ef_A = E\frac{n[mD\sim nA]}{[A^t]} = R_{\text{TC}}\frac{\Delta\alpha}{\alpha^1 r^{\text{ex},2}-\alpha^2 r^{\text{ex},1}}\frac{n}{m}, \tag{10}$$

$$R_{\text{C}} = \frac{[A^t]}{[D^t]} = \frac{1}{R_{\text{TC}}}\frac{\alpha^1 r^{\text{ex},2}-\alpha^2 r^{\text{ex},1}}{\Delta r\delta^1+\Delta\alpha}, \tag{11}$$

where $[A^t]$ and $[D^t]$ are the concentrations of total acceptors and donors; f_D and f_A are the fractions of the donors and acceptors participating in the FRET complexes, respectively, and the calibration factor $R_{\text{TC}} = [D^{\text{ref}}]/[A^{\text{ref}}]$ can be obtained using a tandem construct with a known acceptor/donor stoichiometry, $\Delta\alpha = \alpha^2-\alpha^1$ and $\Delta r = r^{\text{ex},2}-r^{\text{ex},1}$.[17]

In fact, the lux-FRET method proposed by Wlodarczyk et al. has the same Ef_D and R_{C} equations as Eqs. (9) and (11) except that the Ef_A equation is different from Eq. (10) and is given as[11,17]

$$Ef_A = E\frac{[D\sim A]}{[A^t]} = R_{\text{TC}}\frac{\Delta\alpha}{\alpha^1 r^{\text{ex},2}-\alpha^2 r^{\text{ex},1}}, \tag{12}$$

where $[D\sim A]$ is the concentration of the $D\sim A$ pair.

4.2 *spE-FRET: Spectra-Based 2-Channel E-FRET Method*

Based on the measured $\text{count}^i(\lambda)$ ($i=1,2$) spectra at two different excitations, we developed a spectra-based E-FRET method, spE-FRET, to calculate the E and R_{C} values. E was calculated as follows:

$$E = \frac{\text{count}^{1,\text{SE}}(\lambda_2)}{\text{count}^{1,\text{SE}}(\lambda_2)+G(\lambda_1,\lambda_2)\cdot\text{count}^1(\lambda_1)}, \tag{13}$$

where $G(\lambda_1,\lambda_2)$ is a calibration factor under the emission wavelengths of λ_1 and λ_2; $\text{count}^i(\lambda_j)$ is the measured count value at λ_j emission wavelength with λ^i excitation; the superscript SE denotes the sensitized acceptor fluorescence count, and

$$\begin{aligned}\text{count}^{1,\text{SE}}(\lambda_2) = \text{count}^1(\lambda_2)-a[\text{count}^2(\lambda_2)-c\\ \cdot\text{count}^1(\lambda_1)]-d[\text{count}^1(\lambda_1)-b\cdot\text{count}^2(\lambda_2)],\end{aligned} \tag{14}$$

where a, b, c, and d are the crosstalk correction coefficients obtained by using donor-only and acceptor-only samples as follows:

$$\begin{aligned}a &= \text{count}_A^1(\lambda_2)/\text{count}_A^2(\lambda_2)\\ b &= \text{count}_A^1(\lambda_1)/\text{count}_A^2(\lambda_2)\\ c &= \text{count}_D^2(\lambda_2)/\text{count}_D^1(\lambda_1)\\ d &= \text{count}_D^1(\lambda_2)/\text{count}_D^1(\lambda_1),\end{aligned} \tag{15}$$

where the subscript capital letter denotes the sample ("D" denotes donor-only sample and "A" denotes acceptor-only sample). Once these coefficients are determined, all subsequent experiments must be performed under the same measurement conditions. The calibration factor G under this measurement condition can be obtained by using a donor-acceptor tandem construct as follows:

$$G(\lambda_1,\lambda_2) = \frac{\text{count}^{1,\text{SE}}(\lambda_2)-\text{count}^{1,\text{SE-post}}(\lambda_2)}{\text{count}^{1,\text{post}}(\lambda_1)-\text{count}^1(\lambda_1)}, \tag{16}$$

where the superscript "post" denotes the corresponding emission count values after selectively photobleaching partial acceptors.

We can also measure R_C as follows:

$$R_C = \frac{[A^t]}{[D^t]} = \frac{\text{count}^2(\lambda_2) \cdot R}{\text{count}^1(\lambda_1) + \text{count}^{1,SE}(\lambda_2)/G}, \quad (17)$$

where R is the calibration factor for R_C, and $R = (\text{count}^1(\lambda_1) + \text{count}^{1,SE}(\lambda_2)/G)/\text{count}^2(\lambda_2)$ can be obtained using a tandem construct with a 1:1 acceptor-donor stoichiometry under the same measurement conditions.[15]

5 Results and Discussion

5.1 *Spectral Fingerprints of Venus and Cerulean in Living Huh-7 Cells*

In order to use our platform to measure the spectral fingerprints of Cerulean $[e_D(\lambda)]$ and Venus $[e_A(\lambda)]$ in living Huh-7 cells, we first used a standard lamp to calibrate the instrument. Calibration was performed with a halogen tungsten lamp calibrated by a spectrometer (QE65 Pro, Ocean Optics, Florida) that was calibrated by a standard light source (LS-1-CAL, Ocean Optics, Florida). Figure 2(a) showed the reference spectrum $[E(\lambda)]$ of the halogen lamp directly measured by the calibrated QE65 Pro spectrometer, the spectrum $[\text{count}_{\text{lamp}}(\lambda)]$ of the halogen lamp obtained by our spectroscopic widefield fluorescence microscope, and the corresponding spectral sensitivity calibration curve: $K(\lambda) = E(\lambda)/\text{count}_{\text{lamp}}(\lambda)$. The same $K(\lambda)$ curves were obtained at an interval of 3 months [Fig. 2(b)], demonstrating the stability of the spectrometer-microscope platform.

Figure 2(c) showed the spectra of a representative living Huh-7 cell expressing Cerulean (upper two lines) and the corresponding background from cells without expressing FPs (lower two lines), showing that the autofluorescence and background were very low. The mean spectra from cells without expressing FPs under the same measurement conditions were subtracted from the measured fluorescence spectrum. Although 436-nm excitation excited Cerulean more effectively [Fig. 2(c)], the normalized spectrum [Fig. 2(d), black line] was the same as the normalized spectrum with a 405-nm excitation [Fig. 2(d), dashed line], and this spectrum was used as the spectral fingerprint $[e_D(\lambda)]$ of Cerulean. Similarly, the normalized spectrum of Venus in living Huh-7 cells with 436-nm excitation was used as the spectral fingerprint $[e_A(\lambda)]$ of Venus [Fig. 2(e)]. In reality, $e_D(\lambda)$ and $e_A(\lambda)$ were obtained from at least 15 living cells.

Although the measured count(λ) of Cerulean decreased with the decreasing exposure time, normalization showed the same count(λ) spectra (data not shown), indicating that the exposure time of spectrometer did not influence the spectral fingerprints. The shortest exposure time of spectrometer is 8 ms, and in this report, the exposure time is 50 ms.

The stability of the platform is very important for FRET quantification in living cells. Some FRET quantification methods need to calibrate the instrument setup.[9,10,15] For example, three external references are required to determine the instrument setup calibration factor (G) for the E-FRET method[9,15] and the sp-RET method needs to rigorously calibrate the spectral response of the complete optical setup.[10] Although some FRET

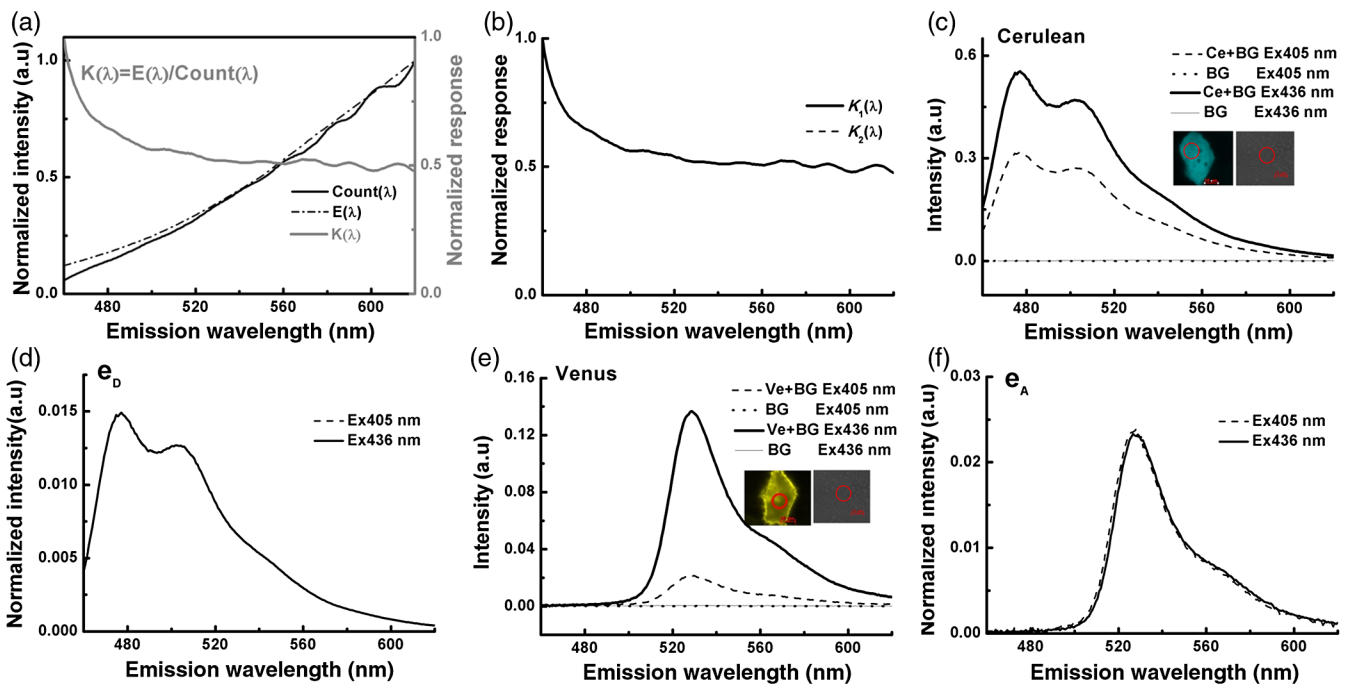

Fig. 2 Spectral fingerprints of Cerulean $[e_D(\lambda)]$ and Venus $[e_A(\lambda)]$ inside living Huh-7 cells. (a) Spectral sensitivity calibration curve $K(\lambda)$ of the spectrometer-microscope platform. (b) Spectral sensitivity calibration curves $K_1(\lambda)$ and $K_2(\lambda)$ measured at intervals of 3 months. (c) Spectra of a representative cell expressing Cerulean and the corresponding background from a cell without expressing fluorescent proteins. Scale bar: 10 μm. (d) Normalized emission spectra of Cerulean inside living cells from at least 15 cells. (e) Same as (c) except for Venus. Scale bar: 10 μm. (f) Same as (d) except for Venus from at least 15 living cells.

quantification methods do not need to calibrate the optical setup, the correction coefficients for removing spectral crosstalks also depend on the stability of the instrument.[11,16,17] All SE-FRET methods need complicated crosstalk correction,[9–11,15–19] and these correction coefficients are intrinsic to the given fluorophores and optical setup as well as the illumination.[1,9,10,17,21,27] In reality, the fluorophores and illumination light are very stable.[9,21,27] Therefore, once these correction coefficients and calibration factors are predetermined for a given choice of fluorophores and instrument, it is not necessary to measure them for every experiment with a steady-state FRET instrument.[1,9,10,19,21,27]

Although our spectrometer-microscope platform is very stable over at least 3 months [Fig. 2(b)], periodic calibration consistently improves the fit quality and the reliability of the measurements. In reality, calibration of the optical setup is very easy, and the normative calibration can be completed in a few minutes. Since the EC is independent of the emission controller, we, here, detected the two spectra at 405- or 436-nm excitation with the same emission channels. Therefore, we used the same calibration curve to correct the measured spectra with different excitations, which is contrary to the sp-RET method proposed by Levy et al.[10]

In fact, the calibration step [Fig. 2(a)] is not mandatory. Spectral fingerprints of the donor [$e_D(\lambda)$] and acceptor [$e_A(\lambda)$] are independent of instrument and illumination, thus they can also be obtained by using other instruments such as a spectrofluorometer.[17] Moreover, once $e_D(\lambda)$ and $e_A(\lambda)$ were determined, we did not need to measure them for every experiment in the specific cell line. In order to insure the accurate measurement of total donor and acceptor emissions, the acquisition range should overlap well with their emission spectra. The spectral ranges chosen in this study fulfill this requirement, covering ~96.3% and ~96.8% of the Cerulean and Venus emission spectra, respectively [Figs. 2(d) and 2(f)].

5.2 *Implementation of mlux-FRET for Measuring the E of C32V in Living Cells*

To use mlux-FRET to measure the E of C32V in living cells, we first measured four reference emission spectra of the Cerulean-only sample and the Venus-only sample, respectively, with two different excitations, and then measured two emission spectra of the C32V sample at the two different excitations under the same measurement conditions. Figure 3(a) showed the images of cells separately expressing Cerulean and Venus with 405-nm (λ^1) and 436-nm (λ^2) excitations, respectively, and the reference spectra inside the living cell indicated by the red circles $\text{count}_D^1(\lambda)(C_D^1)$, $\text{count}_A^1(\lambda)(C_A^1)$ and $\text{count}_D^2(\lambda)(C_D^2)$, $\text{count}_A^2(\lambda)(C_A^2)$ were shown in Figure 3(b). Excitation ratios were determined from the above spectra as: $r^{\text{ex},1} = 2.29$ [Fig. 3(c)] and $r^{\text{ex},2} = 1.21$ [Fig. 3(d)], using quantum yield values of donor and acceptor, $Q_D = 0.62$ and $Q_A = 0.57$.[28] Figure 3(e) showed the images of representative cells expressing C32V under the same measurement conditions as Fig. 3(a), and the spectra and mlux-FRET unmixing (black line) for the live cell indicated by red circles were shown in Figs. 3(f) and 3(g). The estimated parameters were $\alpha^1 = 8.69$, $\alpha^2 = 6.20$, and $\delta^1 = 5.35$. Substitute $m/n = 1$, $r^{\text{ex},i}$, α^i, and δ^i values into Eqs. (9) to (11) to obtain $E = 29.77\%$ and $R_{\text{TC}} = 0.445$. The statistical results from at least 13 cells expressing C32V were $E(E = Ef_D = Ef_A) = 28.67 \pm 0.95\%$ and $R_{\text{TC}} = 0.442 \pm 0.008$.

In reality, we must be very careful when obtaining the reference spectra of Venus with 405-nm excitation due to the very low extinction coefficients of Venus at 405 nm [Fig. 3(a)].

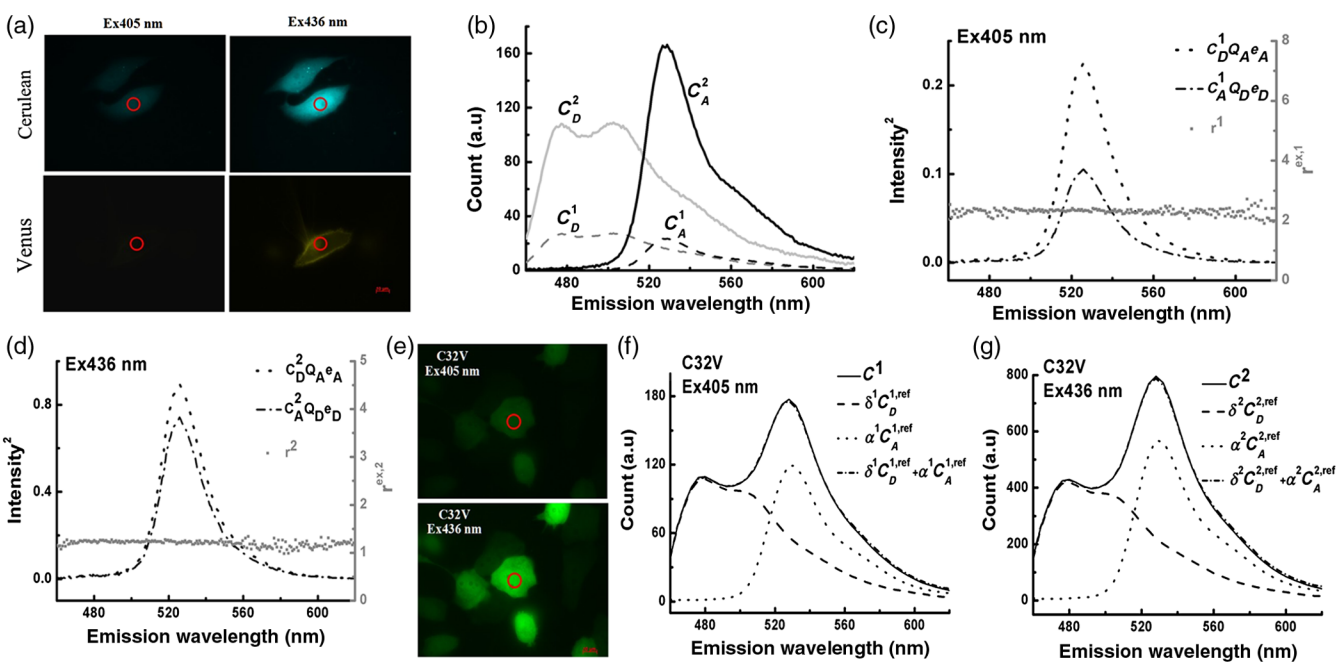

Fig. 3 Implementation of mlux-FRET on the spectrometer-microscope platform for measuring the E of C32V construct inside single living Huh-7 cells. (a) Images of cells separately expressing Cerulean and Venus with 405- or 436-nm excitation. Scale bar: 10 μm. (b) Emission count spectra of Cerulean and Venus inside the living cell indicated by the red circles in (a). (c) and (d) Calculation of excitation ratios $r^{\text{ex},i}$. (e) Image of cells expressing C32V with 405- or 436-nm excitation under the same measurement conditions as the Cerulean-only or Venus-only sample in (a). Scale bar: 10 μm. (f) and (g) Spectral unmixing of C32V with 405-nm (e) or 436-nm (d) excitation.

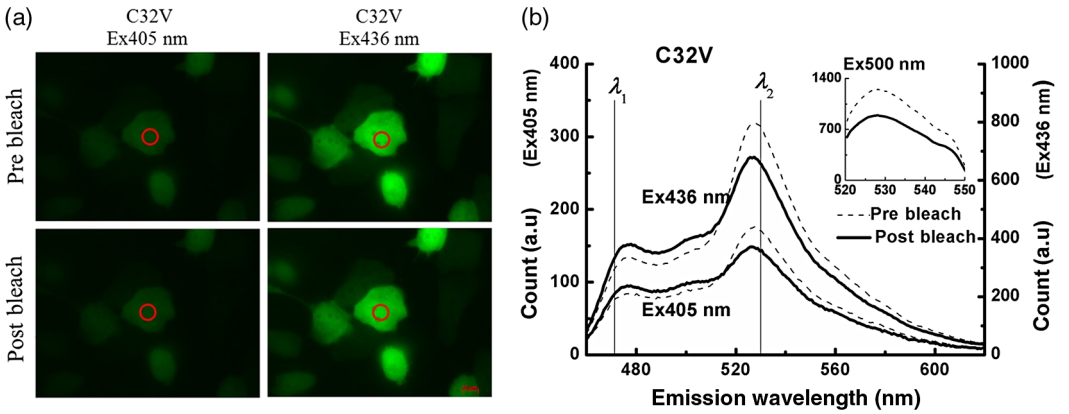

Fig. 4 Implementation of spE-FRET method on the spectrometer-microscope platform for measuring the *E* of C32V construct inside single living Huh-7 cells. (a) Images of cells expressing C32V with 405 nm (left panels) or 436 nm (right panels) excitation before (upper panels) and after (lower panels) partially photobleaching Venus. Scale bar: 10 μm. (b) Count spectra of C32V inside the living cell indicated by red circles in (a). Inset figure: emission spectra of C32V inside the living cells indicated by red circle in (a) before (upper line) and after (lower line) partially photobleaching Venus. λ_1: 470.107 to 470.883 nm and λ_2: 530.452 to 531.223 nm.

Although we can use strong 405-nm excitation to excite Venus, this strong illumination significantly bleached the Venus in C32V (data not shown). Therefore, we must choose cells expressing a high level of Venus as a reference. Although Wlodarczyk et al. used 458- and 488-nm excitations to perform lux-FRET for ECFP-EYFP pair,[17] it is very hard to use a 488 nm laser line to excite Cerulean or ECFP,[10] which was confirmed by the fact that the $r^{\mathrm{ex},2}$ (488-nm excitation) was 0.02, which is much less than the $r^{\mathrm{ex},1} = 2.29$ (458-nm excitation).[17] For 458- and 488-nm excitations, an alternative choice is to use GFP as a donor and YFP or Venus as an acceptor for the implementation of mlux-FRET on a confocal microscope.

The acceptor cross-excitation fraction is intrinsic to the extinction coefficient ratio (γ^i) of the donor to acceptor and their relative concentrations. Different γ^i at two different excitations is necessary for the mlux-FRET method according to Eq. (4). Although the two ratios γ^i ($i = 1, 2$) are related to the cell lines to some extent, they depend mainly on the excitation wavelengths intrinsic to the excitation light source and the transmission properties of the instrument for a given donor-acceptor pair. 405-nm excitation can effectively excite Cerulean/CFP but can hardly excite Venus/YFP, 458-nm excitation can effectively excite both Cerulean/CFP and Venus/YFP, and 488-nm excitation can effectively excite Venus/YFP but hardly excite Cerulean/CFP. Although the γ^1/γ^2 ratio with 458- and 488-nm excitations is 114.5,[9] it is inapplicable to the CFP (Cerulean)–YFP (Venus) pair due to the very low extinction coefficient of CFP (Cerulean) at the 488-nm wavelength. For our spectrometer-microscope platform, 405- and 436-nm excitations ($\gamma^1/\gamma^2 = 1.89$) induced significantly different spectra for C32V, CVC, VCV, and VCVV constructs [Figs. 5(b)–5(e)]. Another better choice, in this view, is the 430- and 445-nm excitations for the CFP (Cerulean)–YFP (Venus) pair.

5.3 *Implementation of spE-FRET for Measuring the E of C32V in Living Cells*

For spE-FRET, we first calculated the spectral crosstalk coefficients according to Eq. (15). We choose 470.107 to 470.883 nm emission data as count(λ_1) and 530.452 to 531.223 nm emission data as count(λ_2). From the measured spectra in Fig. 3(b), the crosstalk correction coefficients for Cerulean and Venus on our spectrometer-microscope platform were $a = 0.142$, $b = 0.001$, $c = 2.650$, and $d = 0.665$. In order to determine the parameter G, we next used a strong 500-nm excitation to selectively bleach partial acceptors inside the same cell as that in Fig. 3(e). Figure 4(a) showed the images of cells in Fig. 3(e) before and after partially photobleaching the acceptor, and the corresponding count spectra of the cell indicated by the red circle in Fig. 4(a) were shown in Fig. 4(b). The degree of PbFRET (x) was 35.46% [inset figure in Fig. 4(b)]. Substitute $\mathrm{count}^1(\lambda_1) = 70.478$, $\mathrm{count}^{1,\mathrm{post}}(\lambda_1) = 78.677$, $\mathrm{count}^1(\lambda_2) = 170.020$, $\mathrm{count}^{1,\mathrm{post}}(\lambda_2) = 143.801$, $\mathrm{count}^2(\lambda_2) = 773.200$, and $\mathrm{count}^{2,\mathrm{post}}(\lambda_2) = 660.001$ [Fig. 4(b)] into Eq. (16) to obtain $G = 1.49$, and the statistical $G = 1.46 \pm 0.05$ from at least 13 living cells. Substitute $G = 1.46$ and these count values into Eqs. (13) and (17) to obtain $E = 27.75\%$ and $R = 0.128$ for the cells indicated by the red circle in Fig. 4(a), and the statistical results from 13 living cells were $E = 28.22 \pm 3.21\%$ and $R = 0.129 \pm 0.007$.

With spE-FRET, the sensitized fluorescence $\mathrm{count}^{i,\mathrm{SE}}(\lambda_2)$ is calculated by subtraction of the major crosstalk components from $\mathrm{count}^1(\lambda_2)$, and the minor crosstalk components from $\mathrm{count}^1(\lambda_1)$ and $\mathrm{count}^2(\lambda_2)$ according to Eq. (14), which is applicable only when the donor channel selectively or mainly collects donor emission.[9] For $\lambda_1 = 500$ to 510 nm and $\lambda_2 = 560.454$ to 561.221 nm, $a = 0.142$, $b = 0.613$, $c = 0.056$, and $d = 0.014$, where b is not ignorable, and the corresponding $G = 0.054 \pm 0.002$ from at least 12 living cells and $E = 23.10\%$, which is much less than 27.75%, further demonstrating our recent study that spE-FRET is also very sensitive to the acceptor emission bleedthrough to the donor channel.[24] It is generally difficult to choose an appropriate optical filter as a donor emission channel to selectively collect donor emission on a conventional widefield fluorescence microscope.[9,22] However, it is very easy to choose a wideband λ_2 (525 to 535 nm) and a narrowband λ_1 (476 to 476.69 nm) to make the crosstalk coefficient $b = 0.0001$ negligible for the Cerulean-Venus pair on our spectrometer-microscope platform. Moreover, choosing 485.624

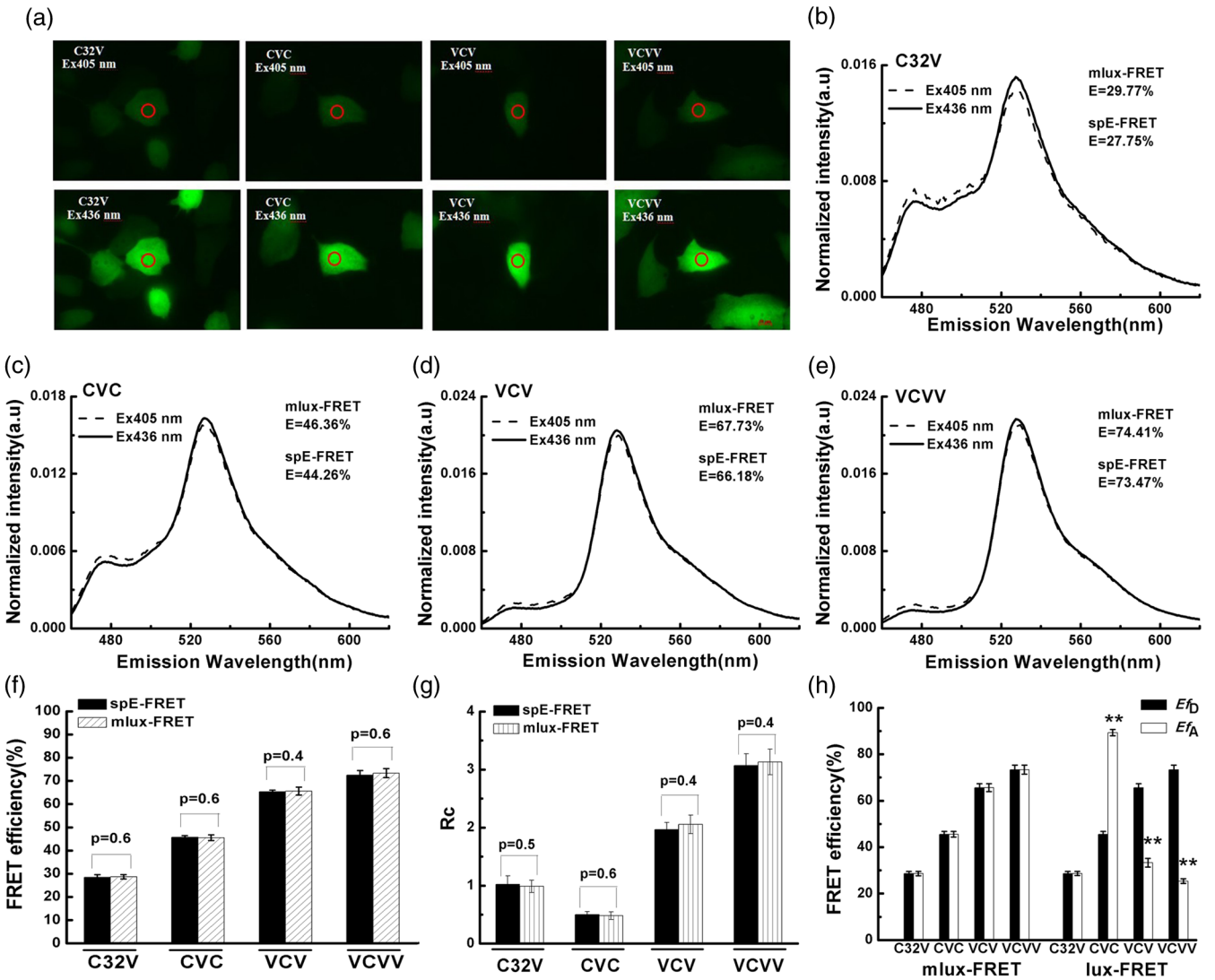

Fig. 5 Implementation of both mlux-FRET and spE-FRET methods on the spectrometer-microscope platform for measuring the E and R_C values of tandem constructs with different acceptor/donor stoichiometries inside single living Huh-7 cells. (a) Images of cells separately expressing C32V, Cerulean-5-Venus-5-Cerulean (CVC), Venus-5-Cerulean-5-Venus (VCV), and Venus-5-Cerulean-5-Venus-6-Venus (VCVV) tandem construct with 405- (upper panels) and 436-nm excitations (lower panels). Scale bar: 10 μm. (b)–(e) Count spectra normalized to unit area of C32V (b), CVC (c), VCV (d), and VCVV (e) constructs inside the cell indicated by red circles in (a) with 405- and 436-nm excitation, respectively. (f) Statistical E values of C32V, CVC, VCV, and VCVV tandem constructs in living Huh-7 cells obtained by mlux-FRET and spE-FRET methods, respectively. (g) Statistical R_C values obtained by spE-FRET and mlux-FRET from Huh-7 cells exclusively expressing CVC, VCV, and VCVV tandem construct. (h) Ef_D and Ef_A of C32V, CVC, VCV, and VCVV tandem constructs with different donor/acceptor stoichiometries in living Huh-7 cells.

to 486.399 nm emission data as count(λ_1), and 520.426 to 550.466 nm emission data as count(λ_2) for the GFP–Venus pair, the corresponding $b = 0.002$ is also negligible.

5.4 *Quantifying Tandem Constructs with Different Acceptor/Donor Stoichiometries in Single Living Huh-7 Cells Using mlux-FRET and spE-FRET Methods*

We next used mlux-FRET and spE-FRET methods to measure the E values of C32V, CVC, VCV, and VCVV constructs inside single living Huh-7 cells. For a live cell expressing the FRET tandem construct, we first measured the spectra at two different excitations. Figure 5(a) showed the images of representative cells expressing C32V, CVC, VCV, and VCVV, respectively, under the same measurement conditions as the Cerulean-only and Venus-only samples in Fig. 3(a). The corresponding normalized spectra of the cell indicated by the red circle in Fig. 5(a) with λ^i excitation and the corresponding values calculated by mlux-FRET and spE-FRET, respectively, were shown in Figs. 5(b)–5(e). The statistical E values from at least 16 live Huh-7 cells in four independent experiments calculated by the two methods showed consistent results for C32V, CVC, VCV, and VCVV constructs, respectively [Fig. 5(f)], and the corresponding R_C values calculated by spE-FRET and mlux-FRET methods were shown in Fig. 5(g).

The Ef_A formalism [Eq. (10)] of mlux-FRET is different from that [Eq. (12)] of lux-FRET. As shown in Fig. 5(h), the Ef_A values calculated by Eq. (10) were consistent with the Ef_D values, while the Ef_A values calculated by Eq. (12) were inconsistent with the Ef_D values except for the C32V construct, verifying the ability of mlux-FRET methods to determine the Ef_A for $mD - nA$ system.

In fact, both the mlux-FRET and spE-FRET methods can be used to measure Ef_D and R_C values of the $mD \sim nA$ construct where the "m" and "n" are unknown. However, a mlux-FRET method can be used to measure the Ef_A value of $mD \sim nA$ construct only when the m/n ratio is known. In reality, the relative concentration of each molecule contained in a biological complex can be predetermined by biotechnology such as flow cytometry, mass spectrometry, or western blotting.[14]

6 Conclusion

In this paper, we developed a spectrometer-microscope platform for simultaneous microscopic imaging and spectral detection in single living cells. The independent excitation and emission controllers make this platform very applicable to implement the most commonly used FRET quantification methods including spFRET and SE-FRET quantification methods in single living cells. A complete FRET quantification measurement on our spectrometer-microscope platform can be completed within 1 to 2 s, and the speed of the current configuration is mainly limited by the manual switch of the two excitation filters. With a programmable excitation and DC system, this platform can monitor the dynamic event inside single living cells on a millisecond scale. In reality, the EC with three filters of this spectrometer-microscope platform can be replaced with a filter wheel with six filters, then the spFRET method based upon the simultaneous unmixing of both excitation and emission spectra[18,19,29] can be readily implemented on this platform. We also developed a modified spFRET method, mlux-FRET, for quantifying the $mD \sim nA$ construct sample in the presence of free donors and acceptors. Moreover, the spE-FRET method we developed here can be readily implemented on this spectrometer-microscope platform for paired FPs with a large spectral overlap such as the GFP-YFP pair.

Acknowledgments

The authors thank Professor S.S. Vogel (NIH/NIAAA) for providing C32V, CVC, VCV, and VCVV plasmids. This work is supported by the National Natural Science Foundation of China (NSFC) (Grant Nos. 81471699 and 61178078) and Guangzhou Science and Technology Plan Project (2014J4100055).

References

1. T. Zal and N. R. J. Gascoigne, "Photobleaching-corrected FRET efficiency imaging of live cells," *Biophys. J.* **86**(6), 3923–3939 (2004).
2. I. L. Medintz et al., "Recent progress in developing FRET-based intracellular sensors for the detection of small molecule nutrients and ligands," *Trends Biotechnol.* **24**(12), 539–542 (2006).
3. B. P. Maliwal et al., "Extending Förster resonance energy transfer measurements beyond 100 Å using common organic fluorophores: enhanced transfer in the presence of multiple acceptors," *J. Biomed. Opt.* **17**(1), 011006 (2012).
4. H. N. Yu et al., "Ma-PbFRET: multiple acceptors FRET measurement based on partial acceptor photobleaching," *Microsc. Microanal.* **19**(1), 171–179 (2013).
5. A. l. Fábián et al., "Strength in numbers: effects of acceptor abundance on FRET efficiency," *ChemPhysChem* **11**(17), 3713–3721 (2010).
6. P. Bojarski et al., "Long-distance FRET analysis: a Monte Carlo simulation study," *J. Phys. Chem. B* **115**(33), 10120–10125 (2011).
7. S. V. Koushik, P. S. Blank, and S. S. Vogel, "Anomalous surplus energy transfer observed with multiple FRET acceptors," *PLoS One* **4**(11), e8031 (2009).
8. A. D. Elder et al., "A quantitative protocol for dynamic measurements of protein interactions by Förster resonance energy transfer-sensitized fluorescence emission," *J. R. Soc. Interface* **6**(S1), S59–S81 (2009).
9. T. Zal and N. R. J. Gascoigne, "Photobleaching-corrected FRET efficiency imaging of live cells," *Biophys. J.* **86**(6), 3923–3939 (2004).
10. S. Levy et al., "SpRET: high sensitive and reliable spectral measurement of absolute FRET efficiency," *Microsc. Microanal.* **17**, 176–190 (2011).
11. A. Zeug et al., "Quantitative intensity-based FRET approaches-a comparative snapshot," *Biophys. J.* **103**(9), 1821–1827 (2012).
12. H. E. Grecco, P. R. Navarro, and P. J. Verveer, "Global analysis of time correlated single photon counting FRET-FLIM data," *Opt. Express* **17**(8), 6493–6508 (2009).
13. H. N. Yu et al., "An empirical quantitative FRET method for multiple acceptors based on partial acceptor photobleaching," *Appl. Phys. Lett.* **100**(25), 253701 (2012).
14. L. L. Zhang et al., "Binomial distribution-based quantitative measurement of multiple-acceptors fluorescence resonance energy transfer by partially photobleaching acceptor," *Appl. Phys. Lett.* **104**, 243706 (2014).
15. H. M. Chen et al., "Measurement of FRET efficiency and ratio of donor to acceptor concentration in living cells," *Biophys. J.* **91**(5), L39–L41 (2006).
16. C. Thaler et al., "Quantitative multiphoton spectral imaging and its use for measuring resonance energy transfer," *Biophys. J.* **89**(4), 2736–2749 (2005).
17. J. Wlodarczyk et al., "Analysis of FRET signals in the presence of free donor and acceptor," *Biophys. J.* **94**(3), 986–1000 (2008).
18. S. Mustafa et al., "Quantitative Förster resonance energy transfer efficiency measurements using simultaneous spectral unmixing of excitation and emission spectra," *J. Biomed. Opt.* **18**(2), 026024 (2013).
19. A. D. Hoppe et al., "N-way FRET microscopy of multiple protein-protein interactions in live cells," *PLoS One* **8**(6), e64760 (2013).
20. H. Düssmann et al., "Single-cell quantification of Bax activation and mathematical modelling suggest pore formation on minimal mitochondrial Bax accumulation," *Cell Death Differ.* **17**(2), 278–290 (2010).
21. A. D. Hoppe, K. Christensen, and J. A. Swanson, "Fluorescence resonance energy transfer-based stoichiometry in living cells," *Biophys. J.* **83**(6), 3652–3664 (2002).
22. T. Zimmermann et al., "Spectral imaging and linear un-mixing enables improved FRET efficiency with a novel GFP2-YFP FRET pair," *FEBS Lett.* **531**, 245–249 (2002).
23. Y. Hiraoka, T. Shimi, and T. Haraguchi, "Multispectral imaging fluorescence microscopy for living cells," *Cell Struct. Funct.* **27**(5), 367–374 (2002).
24. H. L. Li, H. N. Yu, and T. S. Chen, "Partial acceptor photobleaching-based quantitative FRET method completely overcoming emission spectral crosstalks," *Microsc. Microanal.* **18**(5), 1021–1029 (2012).
25. L. Peng et al., "Fourier fluorescence spectrometer for excitation emission matrix measurement," *Opt. Express* **16**(14), 10493–10500 (2008).
26. T. J. Chancellor et al., "Actomyosin tension exerted on the nucleus through nesprin-1 connections influences endothelial cell adhesion, migration, and cyclic strain-induced reorientation," *Biophys. J.* **99**(1), 115–123 (2010).
27. T. Zal, M. A. Zal, and N. R. Gascoigne, "Inhibition of T cell receptor-coreceptor interactions by antagonist ligands visualized by live FRET imaging of the T-hybridoma immunological synapse," *Immunity* **16**(4), 521–534 (2002).
28. N. C. Shaner, P. A. Steinbach, and R. Y. Tsien, "A guide to choosing fluorescent proteins," *Nat. Methods* **2**(12), 905–909 (2005).
29. J. Yuan et al., "Quantitative FRET measurement by high-speed fluorescence excitation and emission spectrometer," *Opt. Express* **18**(18), 18839–18851 (2010).

Liuying Chai received a BS degree in physics from Anyang Normal University, China, in 2012. Her current research interests include fluorescence microscopy and biomedical optics.

Jianwei Zhang received an MS degree in optics from South China Normal University, China. He has three years of experience in fluorescence microscopy and biomedical optics. He is the author of two journal papers.

Lili Zhang received a BS degree in physics from Hubei University, China. She is the author of one journal paper. Her current research interests include fluorescence microscopy and biomedical optics.

Tongsheng Chen received a PhD degree in biomedical engineering from Huazhong University of Science and Technology, China. He has 15 years of experience in fluorescence microscopy and biomedical optics. Since 2005, he has been a full professor of MOE Key Laboratory of Laser Life Science and Institute of Laser Life Science, South China Normal University, Guangzhou, China. He is the author of more than 100 journal papers, and he is also a member of SPIE.